Journal of Computational and Applied Mathematics 431 (2023) 115273

Contents lists available at ScienceDirect

Journal of Computational and Applied Mathematics

journal homepage: www.elsevier.com/locate/cam

Magnus integrators for linear and quasilinear delay differential equations

Ana Arnal *, Fernando Casas, Cristina Chiralt

Institut de Matemàtiques i Aplicacions de Castelló (IMAC) and Departament de Matemàtiques, Universitat Jaume I, E-12071 Castellón, Spain

ARTICLE INFO

Article history:
Received 25 July 2022
Received in revised form 14 February 2023

Keywords:
Non-autonomous linear delay differential equations
Magnus integrators
Characteristic multipliers
Quasilinear problems

ABSTRACT

A procedure to numerically integrate non-autonomous linear delay differential equations is presented. It is based on the use of a spectral discretization of the delayed part to transform the original problem into a matrix linear ordinary differential equation which is subsequently solved with numerical integrators obtained from the Magnus expansion. The algorithm can be used in the periodic case to get both accurate approximations of the characteristic multipliers and the solution itself. In addition, it can be extended to deal with certain quasilinear delay equations.

1. Introduction

We are primarily interested in the numerical integration of a system of linear delay differential equations (DDEs) with a single discrete time delay of the form

$$\begin{aligned} \frac{dx}{dt} &= A(t)\,x(t) + B(t)\,x(t-\tau), \quad t \geq 0 \\ x(t) &= \phi(t), \qquad -\tau \leq t \leq 0, \end{aligned} \tag{1}$$

where $x \in \mathbb{R}^d$, A and B are, in general, time-dependent $d \times d$ matrices and $\phi(t)$ is the initial function. Two cases of special interest arise: when A and B are constant, and when they are periodic of period T. Our purpose is to adapt an integration algorithm originally designed for obtaining numerical approximations to initial value problems defined by non autonomous linear differential equations to this setting. The procedure allows one to get approximations to the solution of (1) for arbitrary $t > 0$ in the general (not necessarily periodic) time-dependent case. It can also be used to analyze the stability of the problem at $t = T$ in the periodic case. The formalism can be readily extended to problems with k distinct delays $0 < \tau_1 < \cdots < \tau_k$,

$$\begin{aligned} \frac{dx}{dt} &= A(t)\,x(t) + \sum_{j=1}^{k} B_j(t)x(t-\tau_j), \quad t \geq 0 \\ x(t) &= \phi(t), \qquad -\tau \leq t \leq 0. \end{aligned} \tag{2}$$

* Corresponding author.
E-mail addresses: ana.arnal@uji.es (A. Arnal), Fernando.Casas@uji.es (F. Casas), chiralt@uji.es (C. Chiralt).

https://doi.org/10.1016/j.cam.2023.115273

Moreover, the procedure is also adapted to quasilinear delay equations of the form

$$\begin{aligned} &\frac{dx}{dt} = A\big(x(t-\tau)\big)\,x(t), \quad t \geq 0 \\ &x(t) = \phi(t), \qquad -\tau \leq t \leq 0. \end{aligned} \tag{3}$$

Eqs. (1) and (2) appear frequently in applications, either as a model of some physical problem or as a tool to analyze its stability when the time evolution of the unknown variable depends not only on the actual state but also on its past values (see e.g. [1,2] and references therein). On the other hand, Eq. (3) has been used to describe SIR-type epidemic models taking into account the latent period, i.e., the time when an individual is infected but is not infective [3]. The well-known scalar delayed logistic equation

$$\frac{dx}{dt} = rx(t)\big(1 - x(t-\tau)\big), \qquad t \geq 0$$

also belongs to this category [4].

Given the relevance of problems (1)–(3), many numerical procedures have been designed over the years for obtaining approximate solutions (see [5] and references therein). Among them, the approximation technique consisting in first converting the DDE (1) when A and B are constant into an abstract Cauchy problem [6,7] is particularly appealing: essentially, it allows one to discretize the corresponding operator by pseudo-spectral collocation and then solve numerically the resulting system of ordinary differential equations (ODEs) by standard methods. This procedure has been used to analyze the stability of linear DDEs, both autonomous [1] and explicitly time-dependent [8], in combination with Chebyshev spectral collocation methods. It is called "continuous time approximation" in [8,9] and, in particular, provides spectral accuracy in the determination of the characteristic roots of the system [1].

The abstract Cauchy problem strategy has been generalized to other classes of nonlinear delay problems such as renewal equations, and systems of coupled renewal equations and delay differential equations [10]. The goal of this technique is to derive systems of ordinary differential equations, analyze their stability and eventually obtain bifurcation diagrams in the space of parameters with the tools already available in the theory of dynamical systems. These include, in particular, the computation of Floquet multipliers [1,11], even for linear time-periodic DDEs with discontinuous coefficients [12,13]. This procedure has also been used to compute periodic solutions, in contrast with the classical approach based on piecewise orthogonal collocation [14].

Our purpose here is to combine the same abstract Cauchy problem strategy with numerical integrators based on the Magnus expansion to carry out the time integration of the resulting system of ordinary differential Eqs. (1) in the non-autonomous case. The time dependence in A and B can be periodic or non-periodic, and the integrator provides by construction the exact solution of the reduced ODE system in the autonomous case. The examples we collect show that this technique, when combined with pseudo-spectral collocation, leads to very accurate results in the determination of Floquet multipliers and periodic trajectories. Even for the quasilinear case (3) it also leads to more accurate approximations to the solution than previous schemes based on the Magnus expansion [3], whereas still preserving qualitative properties of the exact solution.

The plan of the paper is the following. In Section 2 we briefly summarize the continuous time approximation technique for dealing with linear DDEs, whereas the main features of the Magnus expansion and some numerical integrators based on it are reviewed in Section 3. The time integration algorithm is illustrated on several numerical examples in Section 4 and the technique is extended in Section 5 to quasilinear problems, and in particular to an epidemic model with delay. Finally, Section 6 contains some concluding remarks.

2. Continuous time approximation

2.1. Linear DDEs as abstract Cauchy problems

Let us denote by X the state space of continuous functions $C([-\tau, 0], \mathbb{R}^d)$, which is a Banach space with the norm $\|\phi\|_X \equiv \max_{-\tau\leq\theta\leq 0} \|\phi(\theta)\|_\infty$ [1]. If $x_t \in X$ is the state at time t, defined as [15]

$$x_t(\theta) \equiv x(t+\theta), \quad \theta \in [-\tau, 0], \tag{4}$$

then the linear Eq. (1) in the autonomous case can be written as

$$\begin{aligned} &\dot{x} = L x_t, \qquad t \in \mathbb{R} \\ &x_0 = \phi \in X, \end{aligned} \tag{5}$$

where it is assumed that the initial time $t_0 = 0$, the dot denotes the right-hand derivative and $L : X \longrightarrow \mathbb{R}^d$ acts on x_t as

$$L x_t = A\,x(t) + B\,x(t-\tau). \tag{6}$$

In that case, for every $(t_0, \phi) \in \mathbb{R} \times X$, there exists a unique solution of (5) on $[-\tau, +\infty)$, denoted by $x(t;\phi)$ [1]:

$$x(t;\phi) = \begin{cases} \phi(0) + \displaystyle\int_0^t L x_s\, ds, & t \geq 0 \\ \phi(t), & t \in [-\tau, 0]. \end{cases}$$

It is then possible to apply the theory of one-parameter strongly continuous semigroups (also called C_0-semigroups) in this setting. More specifically, it has been shown that the family $\{U(t)\}_{t\geq 0}$ of operators $U(t) : X \longrightarrow X$ associating to the initial function ϕ the state x_t at time $t \geq 0$, i.e, $U(t)\phi = x_t(\cdot;\phi)$, defines a C_0-semigroup of linear and bounded operators on X whose infinitesimal generator is the linear unbounded operator $\mathcal{A} : \mathcal{D}(\mathcal{A}) \subseteq X \longrightarrow X$ given by [16]

$$\begin{aligned} &\mathcal{D}(\mathcal{A}) = \{x \in X \,:\, \dot{x} \in X \ \text{ and } \ \dot{x}(0) = Ax(0) + Bx(-\tau)\} \\ &\mathcal{A}\,x = \dot{x}, \quad x \in \mathcal{D}(\mathcal{A}). \end{aligned} \tag{7}$$

In this way, Eq. (5) can be restated as the linear abstract Cauchy problem

$$\begin{aligned} &\dot{U}(t) = \mathcal{A}\,U(t), \quad t \geq 0 \\ &U(0) = \phi \end{aligned} \tag{8}$$

on the Banach space X, where $U : [0,\infty) \longrightarrow \mathcal{D}(\mathcal{A})$ and the function $U(t) = x_t$ is the unique solution [5].

Typically, problem (5) (or (8)) cannot be solved analytically, so that one has to find a way to get approximations. One possibility consists in discretizing the operator $\mathcal{A}$. This can be done by introducing a mesh $\{\theta_0, \theta_1, \ldots, \theta_N\}$ on the interval $[-\tau, 0]$, with $0 = \theta_0 > \theta_1 > \cdots > \theta_N = -\tau$ and $N \geq 1$. Then, the finite dimensional space $X_N = \mathbb{R}^{d(N+1)}$ is taken as the discretization of X. An element $\Phi = (\Phi_0, \ldots, \Phi_N)^T \in X_N$ can be seen as a function defined on the mesh, with $\Phi_j \in \mathbb{R}^d$, $j = 0, 1, \ldots, N$, being the value at θ_j. As a simple example, let us consider the equispaced mesh $\{\theta_0 = 0, \theta_1 = -h, \ldots, \theta_N = -Nh\}$, with $h = \tau/N$. Then, the $d(N+1)$-dimensional linear system of ODEs

$$\begin{aligned} &\dot{U}_N(t) = \mathcal{A}_N\,U_N(t), \quad t \geq 0 \\ &U_N(0) = \phi_N \end{aligned} \tag{9}$$

with $\phi_N = (\phi(0), \phi(-h), \ldots, \phi(-\tau))^T \in X_N$ and

$$\mathcal{A}_N = \begin{pmatrix} A & 0_d & \cdots & 0_d & B \\ & & D_N \otimes I_d & & \end{pmatrix}$$

approximates the original system (8). Here D_N is a $N \times (N+1)$ matrix corresponding to the particular finite difference scheme one chooses for the integration, I_d is the $d \times d$ identity matrix and $\otimes$ denotes the tensor product [5–7]. For instance, if a first-order forward difference approximation is used, then

$$D_N = \frac{1}{h}\begin{pmatrix} -1 & 1 & & & & \\ & -1 & 1 & & & \\ & & \ddots & \ddots & & \\ & & & -1 & 1 & \\ & & & & -1 & 1 \end{pmatrix}.$$

A much more accurate description can be achieved by considering instead a pseudo-spectral differentiation method based on Chebyshev collocation points. In this approach one takes the $N+1$ Chebyshev points

$$t_j = \cos\frac{j\pi}{N}, \qquad j = 0, \ldots, N$$

on the interval $[-1, 1]$ and the corresponding shifted points $\theta_j = (t_j - 1)\tau/2$ as the mesh in $[-\tau, 0]$. Then,

$$\phi_N = (\phi(\theta_0), \phi(\theta_1), \ldots, \phi(\theta_N))^T \in \mathbb{R}^{d(N+1)} \tag{10}$$

and the matrix $\mathcal{A}_N$ is obtained as follows. First, one considers the standard $(N+1)\times(N+1)$ spectral differentiation matrix D for the Chebyshev collocation points. The entries of D can be found, e.g. in [17, p. 53]. Then one constructs the matrix $\mathbb{D} = D \otimes I_d$, and finally $\mathcal{A}_N$ is formed from $\mathbb{D}$ by replacing its first d rows by zeros and replacing the $d \times d$ left upper corner by A and the $d \times d$ right upper corner by B. In other words,

$$\mathcal{A}_N = \begin{pmatrix} A & 0_d & \cdots & 0_d & B \\ & & \frac{2}{\tau}[\mathbb{D}^{(d+1,d(N+1))}] & & \end{pmatrix}. \tag{11}$$

Here $[\mathbb{D}^{(d+1,d(N+1))}]$ denotes the submatrix obtained by taking the rows $d+1, \ldots, d(N+1)$ from $\mathbb{D}$, whereas the factor $2/\tau$ accounts for rescaling from the interval $[-1, 1]$ to $[-\tau, 0]$ [8]. In particular, if $d = 1$ and $N = 4$, one has

$$\mathcal{A}_4 = \frac{2}{\tau}\begin{pmatrix} \frac{\tau}{2}A & 0 & 0 & 0 & \frac{\tau}{2}B \\ 1+\frac{\sqrt{2}}{2} & -\frac{\sqrt{2}}{2} & -\sqrt{2} & \frac{\sqrt{2}}{2} & -\frac{1}{2+\sqrt{2}} \\ -\frac{1}{2} & \sqrt{2} & 0 & -\sqrt{2} & \frac{1}{2} \\ \frac{1}{2+\sqrt{2}} & -\frac{\sqrt{2}}{2} & \sqrt{2} & \frac{\sqrt{2}}{2} & -1-\frac{\sqrt{2}}{2} \\ -\frac{1}{2} & \frac{4}{2+\sqrt{2}} & -2 & \frac{4}{2-\sqrt{2}} & -\frac{11}{2} \end{pmatrix},$$

where now A and B are scalars. In this way, one ends up with the $d(N+1)$-dimensional initial value problem defined by (9), with coefficient matrix (11) and initial condition (10). By solving this system in the interval $[0, \tau]$, one constructs

a vector $U_N(\tau)$ whose entries constitute approximations to the solution of the DDE (5) at times $\theta_j^1 \equiv \tau + \theta_j$, namely $(U_N(\tau))_j \approx x(\tau + \theta_j)$. The solution of (9) is obtained by evaluating $U_N(\tau) = \exp(\tau \mathcal{A}_N)\phi_N$ and the first d components of $U_N(\tau)$ provide the solution at $t = \tau$, the next d components approximate the solution at $t = \tau + \theta_1 = (1 + t_1)\frac{\tau}{2}$, etc.

If N is sufficiently large, by applying this procedure one gets in fact spectral accuracy when computing the eigenvalues of the approximate matrix $\mathcal{A}_N$: as shown in [1], the eigenvalues of $\mathcal{A}_N$ converge to the eigenvalues of the operator $\mathcal{A}$ faster than $\mathcal{O}(N^{-r})$ for any $r > 0$. Of course, the number of elements in the spectrum of $\mathcal{A}$ that are approximated by elements of the spectrum of $\mathcal{A}_N$ increases with the value of N, and the eigenvalues which are closest of the origin are better approximated.

If one is interested in obtaining approximate solutions of the DDE (5) for $t > \tau$, then the procedure consists in taking successive intervals $[\tau, 2\tau]$, $[2\tau, 3\tau]$, etc. and proceed as in the method of steps, taking as initial condition the approximation obtained in the previous interval. Thus, if we denote $\theta_j^i \equiv i\tau + \theta_j = i\tau + \frac{(t_j-1)\tau}{2}$, to get approximations in the $(i+1)$-th interval $[i\tau, (i+1)\tau]$, $i \geq 1$, we have to solve (9) with the initial condition $U_N(i\tau)$ obtained by integrating on the previous ith interval. If, on the other hand, we want to get approximations at a particular time $t \in (i\tau, (i+1)\tau)$, then an interpolation can be carried out based on the values obtained at the Chebyshev points in the interval.

2.2. Linear periodic DDEs

Whereas in the autonomous case, the infinitesimal generator approach allows one to get accurate approximations to the eigenvalues and the solution of (1), and even obtain rigorous convergence estimates, the situation is far more complicated when matrices A and B in (1) depend explicitly on time. One could analogously try to describe the time evolution of the linear DDE through a Cauchy problem defined for an abstract ODE, but in that case one has to introduce a 2-parameter family of operators called *evolution family* as solutions for abstract Cauchy problems of the form [18, Chapter 3]

$$\dot{y}(t) = \mathcal{A}(t)\, y(t), \quad y(s) = z \in \mathcal{D}(\mathcal{A}(s)), \quad t \geq s, \tag{12}$$

where the domain $\mathcal{D}(\mathcal{A}(s))$ of the operator $\mathcal{A}(s)$ is assumed to be dense in X. Specifically, a family $\{U(t,s)\}_{t \geq s}$ of linear and bounded operators on X is called an evolution family if

(i) $U(t,s) = U(t,\nu)U(\nu,s)$ and $U(s,s) = I$ for all $t \geq \nu \geq s$; and
(ii) for each $\phi \in X$, the function $(t,s) \mapsto U(t,s)\phi$ is continuous for $t \geq s$.

The abstract Cauchy problem (12) is called *well-posed* if there exists an evolution family $\{U(t,s)\}_{t \geq s}$ that solves (12), i.e., if for each $s \in \mathbb{R}$, there exists a dense subset $Y_s \subseteq \mathcal{D}(\mathcal{A}(s))$ such that, for each $y_s \in Y_s$ the function $t \mapsto y(t) \equiv U(t,s)y_s$, for $t \geq s$, is differentiable, $y(t) \in \mathcal{D}(\mathcal{A}(t))$ and (12) holds [16,18].

It has been shown that the non-autonomous Cauchy problem (12) is well-posed if and only if there exists a unique evolution family $\{U(t,s)\}_{t \geq s}$ solving (12) [16,19]. If the well-posedness of the problem has been established (which in some cases is far from trivial [16,18,20]), then the unique solution has the form

$$y(t) = U(t,s)z \qquad \text{for} \qquad t \geq s.$$

In the particular case of periodic problem with period T,

$$\begin{aligned} &\dot{x} = L(t)\, x_t, \quad t \geq s \\ &x_s = \phi, \end{aligned} \tag{13}$$

the evolution operator $U(t,s)\phi = x_t(\cdot; s, \phi)$ verifies in addition that $U(t+T, s) = U(t,s)U(s+T,s)$ for all $t \geq s$, and it is the so-called monodromy operator $U(T,0)$ what is the central object of study to determine the stability of the system. It can be shown that the spectrum of $U(T,0)$ is an at most countable compact set of $\mathbb{C}$ with zero as the only possible accumulation point. Moreover, any eigenvalue $\mu \neq 0$ belongs to the point spectrum, and is called a characteristic multiplier of Eq. (1) [15]. In particular, the zero solution of (13) is uniformly asymptotically stable if and only if all the characteristic multipliers are such that $|\mu| < 1$ [1,15]. In any event, the solution $y(t)$ (corresponding to $x(t)$ in (1)) has to be approximated at certain values of t.

Whereas in [1] a pseudo-spectral collocation method is applied directly to discretize the monodromy operator $U(T,0)$ and to compute approximations to the characteristic multipliers of (1), in this paper we proceed formally as in the case of autonomous problems. In other words, we take $N+1$ Chebyshev nodes in the interval $[-\tau, 0]$, replace X by the finite dimensional space X_N and the abstract Cauchy problem (12) by

$$\begin{aligned} &\dot{U}_N(t) = \mathcal{A}_N(t)\, U_N(t), \quad t \geq 0 \\ &U_N(0) = \phi_N, \end{aligned} \tag{14}$$

where now

$$\mathcal{A}_N(t) = \begin{pmatrix} A(t) & 0_d & \cdots & 0_d & B(t) \\ & & \frac{2}{\tau}[\mathbb{D}^{(d+1,d(N+1))}] & & \end{pmatrix} \tag{15}$$

is a periodic matrix of period T and the initial vector is the discretization of the function $\phi(t)$ at the shifted Chebyshev points,

$$\phi_N = (\phi(\theta_0), \phi(\theta_1), \ldots, \phi(\theta_N))^T \in \mathbb{R}^{d(N+1)}. \tag{16}$$

This problem is then numerically integrated to get approximations to the solution over the interval $[0, \tau]$, specifically at the times determined by the Chebyshev points. The particular class of numerical schemes used for that will be introduced in the next section. Depending on the value of N we get approximations at more points in $[0, \tau]$. Once the approximation at $t = T$ is obtained, then the monodromy operator is available, so that one readily determines the first $d(N+1)$ characteristic multipliers of Eq. (1) [8].

We remark once again that by following this procedure we have set aside all the technical issues related to the existence of the evolution family of operators for the abstract Cauchy problem (12). An informal theoretical justification of the present approach is provided for periodic delay equations in the Appendix of [8].

3. Numerical integration of linear DDEs

3.1. Numerical integrators based on the Magnus expansion

One is then confronted with the numerical time integration of the non-autonomous initial value problem (14)–(16) defined in the finite dimensional space X_N. This of course can be done by applying several numerical integrators, such as Runge–Kutta or multistep methods. Among them, numerical methods based on the Magnus expansion are particularly appropriate for linear systems, resulting in very efficient schemes that, in addition, preserve important qualitative properties of the continuous system [21]. It makes sense, then, trying to combine the spectral accuracy provided by the Chebyshev collocation points with Magnus integrators to get accurate approximations.

Magnus's approach to solve the general linear differential equation

$$\dot{y}(t) = \hat{A}(t)\, y(t), \qquad y(0) = y_0, \tag{17}$$

where $\hat{A}(t)$ is a $m \times m$ matrix and $y \in \mathbb{R}^m$, consists in expressing the solution as an exponential $y(t) = \exp(\Omega(t))y_0$, and determining the equation satisfied by $\Omega(t)$. Specifically, it can be shown that

$$\dot{\Omega} = \sum_{k=0}^{\infty} \frac{B_k}{k!} \mathrm{ad}_{\Omega}^k(\hat{A}(t)), \qquad \Omega(0) = 0, \tag{18}$$

where B_k are the Bernoulli numbers and $\mathrm{ad}_{\Omega}(\hat{A}) = [\Omega, \hat{A}] = \Omega\,\hat{A} - \hat{A}\,\Omega$, $\mathrm{ad}_{\Omega}^k(\hat{A}) = [\hat{A}, \mathrm{ad}_{\Omega}^{k-1}(\hat{A})]$. Eq. (18) is then solved by applying Picard fixed point iteration after integration. This results in an infinite series for Ω,

$$\Omega(t) = \sum_{k=1}^{\infty} \Omega_k(t), \qquad \text{with} \qquad \Omega_k(0) = 0, \tag{19}$$

whose terms are increasingly complex expressions involving time-ordered integrals of nested commutators of $\hat{A}$ evaluated at different times [22,23]. In particular,

$$\begin{aligned} \Omega_1(t) &= \int_0^t \hat{A}(t_1) dt_1, \\ \Omega_2(t) &= -\frac{1}{2} \int_0^t dt_1 \int_0^{t_1} dt_2 \, \left[\hat{A}(t_2), \hat{A}(t_1)\right]. \end{aligned} \tag{20}$$

The expansion is guaranteed to converge at least for $t \in [0, t_c)$ such that

$$\int_0^{t_c} \|\hat{A}(s)\|_2 \, ds < \pi\,.$$

By appropriately truncating the series and approximating the integrals by suitable quadratures, it is then possible to design numerical integration schemes for approximating the solution of Eq. (17) in a given interval $[0, t_f]$ [21,22]. As usual, the integration interval is divided into M steps such that (19) converges in each subinterval $[t_k, t_{k+1}]$, $k = 0, \ldots, M$, with $t_M = t_f$ and length $h = t_f/M$. Then, an approximation to the solution of (17) of order $2p$ is achieved by computing

$$y(t_{k+1}) \approx y_{k+1} = \exp(\Omega^{[2p]}(h))\, y_k, \qquad k = 0, 1, \ldots, M-1, \tag{21}$$

where $\Omega^{[2p]}(h) = \Omega(h) + \mathcal{O}(h^{2p+1})$. Since the construction procedure is detailed in Refs. [22,24], here we only collect specific integration schemes of order $2p = 2, 4, 6$.

Order 2. A 2nd-order scheme is attained by approximating Ω_1 by the midpoint rule. It reads

$$y_{k+1} = \exp(h\hat{A}(t_k + h/2))\, y_k, \qquad k = 0, \ldots, M-1 \tag{22}$$

and is also known as the exponential midpoint rule.

Order 4. If we take the 2 points Gauss–Legendre quadrature rule and compute

$$A_1 = \hat{A}\left(t_k + \left(\frac{1}{2} - \frac{\sqrt{3}}{6}\right)h\right), \qquad A_2 = \hat{A}\left(t_k + \left(\frac{1}{2} + \frac{\sqrt{3}}{6}\right)h\right),$$

then the scheme

$$\begin{aligned} \Omega^{[4]}(h) &= \frac{h}{2}(A_1 + A_2) - h^2\frac{\sqrt{3}}{12}[A_1, A_2] \\ y_{k+1} &= \exp(\Omega^{[4]}(h))\, y_k \end{aligned} \tag{23}$$

renders an integration method of order 4 for Eq. (17).

Order 6. By evaluating the matrix $\hat{A}$ at the Gauss–Legendre collocation points

$$A_1 = \hat{A}(t_k + c_1 h), \qquad A_2 = \hat{A}(t_k + c_2 h), \qquad A_3 = \hat{A}(t_k + c_3 h),$$

with $c_1 = 1/2 - \sqrt{15}/10$, $c_2 = 1/2$, $c_3 = 1/2 + \sqrt{15}/10$, we form the quantities

$$\alpha_1 = hA_2, \qquad \alpha_2 = \frac{\sqrt{15}h}{3}(A_3 - A_1), \qquad \alpha_3 = \frac{10h}{3}(A_3 - 2A_2 + A_1),$$

and finally

$$\begin{aligned} C_1 &= [\alpha_1, \alpha_2] \\ C_2 &= -\frac{1}{60}[\alpha_1, 2\alpha_3 + C_1] \\ \Omega^{[6]}(h) &= \alpha_1 + \frac{1}{12}\alpha_3 + \frac{1}{240}[-20\alpha_1 - \alpha_3 + C_1, \alpha_2 + C_2] \\ y_{k+1} &= \exp(\Omega^{[6]}(h))\, y_k. \end{aligned} \tag{24}$$

Then we end up with an integrator of order 6 requiring only the evaluation of $\hat{A}$ at three different times and the computation of 3 commutators.

These schemes have shown to be more efficient than standard integrators such as Runge–Kutta methods, even when the evaluation of the exponential of a matrix is required at each step [24]. In this respect, we note that several algorithms have been recently proposed to reduce the computational cost of the exponential matrix [25], especially in the context of exponential integrators [26]. These will be incorporated into our procedure.

3.2. Integration algorithm

We have now all the tools required to formulate a practical algorithm for the numerical integration of the linear DDE (1) in the interval $t \in [0, \tau]$, for generic (sufficiently smooth) $d \times d$ matrices $A(t)$, $B(t)$ and an initial function $\phi(t)$. It can be summarized as follows:

1. Choose an integer N and form the spectral differentiation matrix $\mathbb{D}$ associated with the $N+1$ Chebyshev collocation points on the interval $[-1, 1]$.
2. Construct the $d(N+1) \times d(N+1)$ matrix $\mathcal{A}_N(t)$ of Eq. (15).
3. Form the $d(N+1)$-dimensional vector $U_N(0)$, whose elements are the values of the initial function ϕ at the shifted Chebyshev collocation points on the interval $[-\tau, 0]$.
4. Choose an integer M, the step size $h = \tau/M$ and construct the numerical solution $\widetilde{U}_N(Mh)$ of the initial value problem (14)–(16) at the final time $t = \tau$ by applying one of the numerical integrators of Section 3.1 obtained from the Magnus expansion. In all of them, $\exp(\Omega^{[2p]})$ is computed with the algorithm presented in [25] based on Taylor polynomials.
5. The vector $\widetilde{U}_N(Mh)$ provides an approximation to $U_N(\tau)$ of order of convergence $2p$, i.e.,

   $$\widetilde{U}_N(Mh) = U_N(\tau) + \mathcal{O}(h^{2p+1}), \qquad p = 1, 2, 3,$$

   and thus also approximates the solution of Eq. (1) at times $\tau + \theta_j$, $j = 0, \ldots, N$.

As pointed out before, if the solution has to be computed at times $t > \tau$, the same process can be applied in any interval $[i\tau, (i+1)\tau]$, $i \geq 1$, taking as initial condition the approximation at the end of the previous interval, $\widetilde{U}_N(Mh)$. The matrix $\mathcal{A}_N(t)$ has to be formed again, of course, but the only difference with respect to the previous interval lies in the time-dependent part (i.e., in $A(t)$ and $B(t)$).

The procedure has thus three main ingredients: (a) the original DDE is reformulated as an abstract Cauchy problem in the Banach space X; (b) this problem is then discretized by a pseudo-spectral method, thus leading to an initial value problem defined in a finite-dimensional space X_N, and (c) finally a Magnus integrator is applied to solve numerically the

resulting finite-dimensional non-autonomous ordinary differential equation. In this sense, the algorithm thus combines the advantages of both spectral and Magnus methods.

Notice, in particular, that the procedure critically depends on the parameters N (related to the discretization of the delayed part) and M (leading to the step size h in the time numerical integration), and finally also on the order of accuracy of the Magnus integrator. These parameters can be chosen according with the required accuracy, and are clearly related, although a precise characterization of this relationship is still lacking. The situation closely resembles what happens when a Magnus integrator is used to integrate in time a partial differential equation previously discretized in space: one has to adjust M to provide an accuracy consistent with the scheme used for the space discretization [27,28].

In this respect it is worth noticing that the Magnus expansion provides the exact solution of the initial value problem (14)–(16) in the autonomous case (i.e., when the matrices A and B in (1) are constant). This feature can be used to choose the number of collocation points N leading to the required accuracy in the general case simply by freezing t at one specific time. Once a particular N has been selected, the number of subdivisions M and the order of the Magnus integrators can be fixed according with some specified tolerance. The order and the step size can even be changed from one particular interval $[i\tau, (i+1)\tau]$ to the next [29].

If the number of nodes N of the spectral discretization is sufficiently large, then the algorithm has the usual properties exhibited by standard Magnus integrators applied to non-autonomous linear differential equations concerning stability, convergence and error propagation [21,22,24].

In the periodic case, one can use this procedure to compute the fundamental matrix of system (14) at time $t = T \geq \tau$, and its eigenvalues. Then, they provide approximations to the first $d(N+1)$ characteristic multipliers of the DDE (1). As in the autonomous case, the eigenvalues that are closest to its minimum value (in absolute value) are better approximated.

It is worth remarking that, whereas the previous algorithm only deals with one delay, it can be easily generalized to the case of multiple discrete delays, i.e., to solve numerically Eq. (2) by applying any of the alternatives proposed by [8]: either by fitting a single Chebyshev polynomial through the entire delay interval $[-\tau_k, 0]$ or by considering a different Chebyshev polynomial of different degree in every interval $[-\tau_k, -\tau_{k-1}]$, $[-\tau_{k-1}, -\tau_{k-2}]$, etc.

4. Numerical examples

Next we illustrate the algorithm presented in Section 3 in practice on several examples, both for computing the first characteristic multipliers of the problem and also for getting numerical approximations to the exact solution. For convenience, we denote the previous Magnus integrators of order 2, 4 and 6 as M2, M4 and M6, respectively.

Example 1: a scalar periodic equation. As a first illustration we take the admittedly simple non-autonomous one-dimensional equation with 2π-periodic coefficients and delay $\tau = \frac{\pi}{2}$

$$\dot{x}(t) = \cos(t)\, x(t) - \mathrm{e}^{\sin t + \cos t}\, x(t - \frac{\pi}{2}). \tag{25}$$

It is taken from [1] and arises when linearizing the nonlinear autonomous DDE

$$\dot{z}(t) = -\log\left(z\left(t - \frac{\pi}{2}\right)\right) z(t). \tag{26}$$

around its periodic solution $z(t) = \exp(\sin t)$. It is a simple exercise to check that $x(t) = \dot{z}(t) = \mathrm{e}^{\sin t}\cos t$ is indeed a solution of (25), so that $\mu = 1$ is a characteristic multiplier [1]. We can therefore check the accuracy of the algorithm by computing both the spectrum of the monodromy matrix and the numerical approximation to the exact solution by integrating Eq. (25) with initial function $\phi(t) = \mathrm{e}^{\sin t}\cos t$.

The first test is devoted to check the accuracy in the determination of the characteristic multiplier $\mu = 1$. This is done by computing the monodromy matrix through the numerical integration of the matrix system

$$\dot{Y} = \mathcal{A}_N(t) Y, \qquad Y(0) = I$$

associated with (14)–(15) until the final time $t_f = 2\pi$, i.e., in the interval $[0, 4\tau]$, with the presented Magnus integrators, and then by obtaining its eigenvalues . We then compute the difference between the first eigenvalue and $\mu = 1$ as a function of M (the number of subdivisions in each interval $[i\tau, (i+1)\tau]$) for different values of N (the number of collocation points). In this way, we obtain the results collected in Fig. 1, with $N = 10$ (left diagram) and $N = 20$ (right panel). The order of approximation of M2 and M4 is clearly visible in the figure, whereas the higher accuracy of M6 is only visible for sufficiently large N and M. Here and in the sequel, for illustration, we indicate the theoretical order by including small segments with the corresponding slope in the graphs.

Notice that the main limiting factor for accuracy in the left panel is the small number of collocation points: doubling the value of N, from 10 to 20, allows us to decrease the error by more than 5 orders of magnitude. In this respect, it is worth mentioning that with the procedure proposed in [1], $N = 40$ collocation points are required to render similar errors as those achieved here with $N = 20$.

In our second experiment we check the accuracy in solving the problem (25) for long times by computing approximations to the exact solution. Specifically, we integrate until the much larger final time $t_f = 100\pi$ with M2, M4 and M6 for

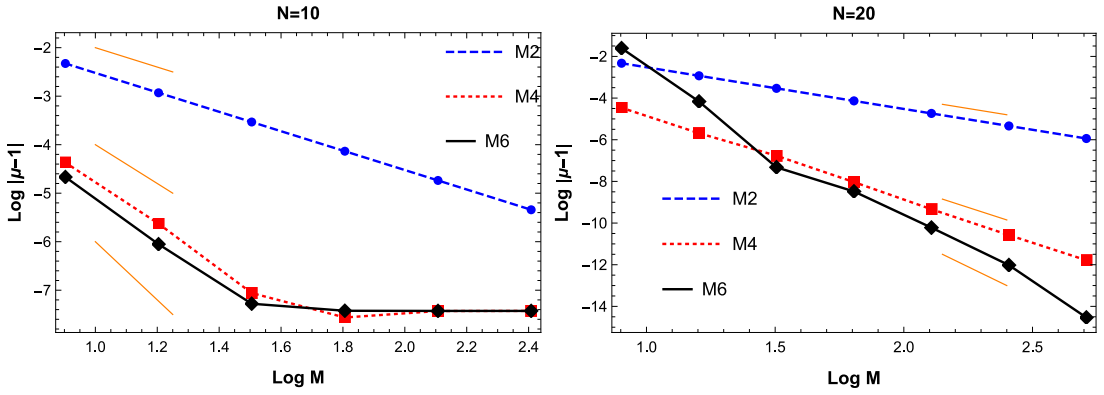

Fig. 1. Error in the dominant characteristic multiplier $\mu = 1$ for the problem (25) obtained with Magnus integrators M2, M4 and M6 as a function of M with two different values for the number of collocation points: $N = 10$ (left) and $N = 20$ (right). The small segments correspond to the theoretical order 2, 4 and 6.

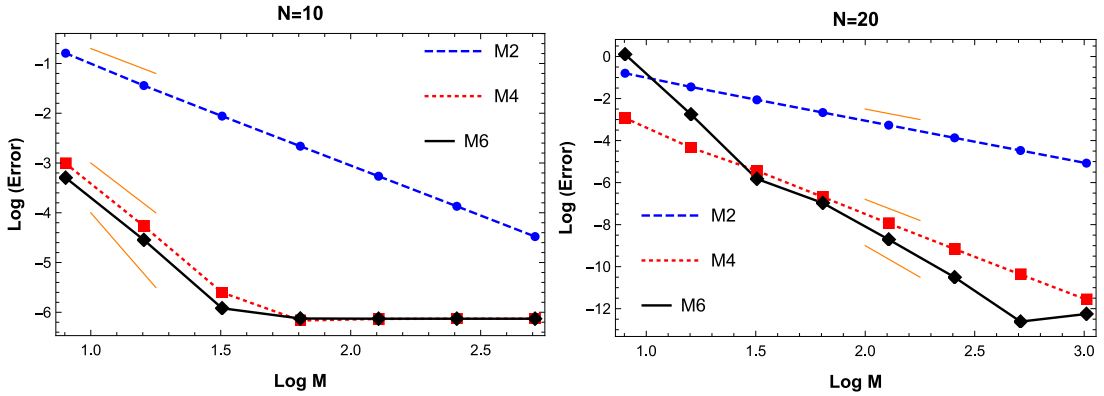

Fig. 2. Mean error (27) in the solution $x(t) = e^{\sin t}\cos t$ of (25) obtained with Magnus integrators M2, M4 and M6 as a function of M with two different values for the number of collocation points: $N = 10$ (left) and $N = 20$ (right). Final time: $t_f = 100\pi$.

different values of M and compute the mean error of the solution in the last interval $[199\tau, 200\tau]$,

$$E = \frac{1}{N+1}\sum_{j=0}^{N} |x(t_j) - (U_N)_j|. \tag{27}$$

Here $x(t_j) = e^{\sin t_j}\cos t_j$, $t_j = 200\tau + \theta_j$ and U_N are the approximations obtained with each integrator. The results are displayed in Fig. 2 for $N = 10$ (left) and $N = 20$ (right) collocation points. The same notation as in Fig. 1 has been used for each method. Here again, the higher order of M6 is already visible with only $N = 20$ collocation points, and the quality of the approximation does not degrade even if long time integrations are considered. Notice the close similarity between the results exhibited in Figs. 1 and 2.

Example 2: delayed Mathieu equation. The DDE we consider next is

$$\ddot{x}(t) + (\delta + \varepsilon\cos t)x(t) = b\,x(t-\tau), \tag{28}$$

where δ, ε and b are real parameters. The case in which the time delay τ is equal to the principal period 2π has been thoroughly studied in the literature, especially with respect to its stability [2], and so we also fix $\tau = 2\pi$ here. Eq. (28) includes both the effects of time delay and the presence of parametric forcing, and appears in relevant mechanical engineering problems (see [2] and references therein).

The delayed Mathieu Eq. (28) can be considered as a prototypical example of a linear delay equation and as such it can be used as a suitable test bench for different numerical procedures aimed at computing periodic orbits, Floquet multipliers, bifurcation diagrams in the space of parameters, etc. It is not our purpose to provide a comprehensive analysis of this problem, but only to illustrate some of the features of the Magnus integrators when solving the initial value problem resulting from a pseudo-spectral discretization of the original equation. In this way we may add yet another tool to the arsenal already available to analyze all these issues, as shown e.g. in [10,12–14,30] and references therein.

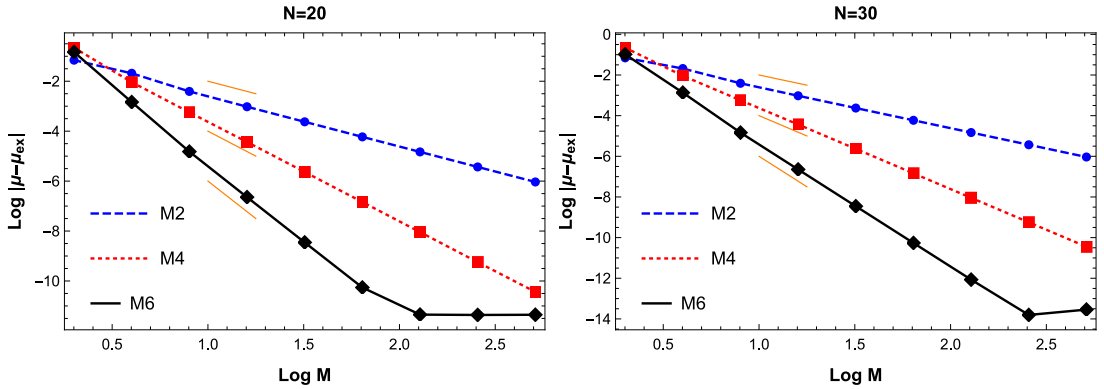

Fig. 3. Error in the first characteristic multiplier μ_{ex} for the delayed Mathieu equation (28) obtained with Magnus integrators M2, M4 and M6 as a function of M for $N = 20$ (left) and $N = 30$ (right). The values of the parameters are: $\delta = 1.5$, $\varepsilon = 0.5$, $b = -0.2$.

Eq. (28) is transformed into a system of the form (1) with $d = 2$ and matrices

$$A(t) = \begin{pmatrix} 0 & 1 \\ -(\delta + \varepsilon \cos t) & 0 \end{pmatrix}, \qquad B = \begin{pmatrix} b & 0 \\ 0 & 0 \end{pmatrix},$$

to which the previous algorithm can be readily applied. In our first test we fix the parameters to the values $\delta = 1.5$, $\varepsilon = 0.5$ and $b = -0.2$. By using the Floquet technique proposed in [31], it can be seen that one of the characteristic multipliers is given by $\mu_{ex} = \alpha + i\beta$, with

$$\alpha = 0.22751840350292177638239482513$$
$$\beta = 1.41717517421553068345788187573 7$$

and 30 digits of accuracy. This is taken as the reference value to compare with our procedure. As in the previous example, we compute the corresponding monodromy matrix with Magnus integrators M2, M4 and M6 for different values of the discretization parameters N and M. We then determine its first eigenvalue μ_1 and the error $|\mu_1 - \mu_{ex}|$ by fixing N and several values of M. The corresponding results are depicted in Fig. 3 (in a log–log scale) when $N = 20$ (left) and $N = 30$ (right) as a function of M. Again, the order of each scheme is clearly visible, with M6 providing the most accurate approximations for all the values of M considered. Here also the number of collocation points N determines the maximal accuracy one can get. For comparison, with the numerical technique proposed in [1] (based on the direct discretization of the evolution operator) one gets also round-off accuracy with $N = 30$, whereas the error achieved with $N = 20$ is $\approx 3.1 \cdot 10^{-9}$. Notice that, even with a time step as large as $h = \tau/2$ (or $M = 2$), the results show the expected order of convergence, and are not affected by any possible loss of stability of the time integrators.

To check how the errors in the numerical solution evolve with time, for our next experiment we take as initial condition $\phi(t) = t$ and integrate the initial value problem (14)–(16) until the final time $t_f = 10\tau = 20\pi$ with a fixed value for both discretization parameters, $N = 40$, $M = 200$. As a measure of the error we compute the quantity

$$E_i = \frac{1}{N+1} \sum_{j=0}^{N-1} |x(t_j) - (U_N)_{2j+1}|, \qquad \text{with} \qquad t_j \in [i\tau, (i+1)\tau]. \tag{29}$$

We call E_i the mean error in each subinterval, where the reference solution $x(t)$ is taken as the output of the function `NDSolve` of *Mathematica* with a very stringent tolerance. Notice that, since $d = 2$, the odd components of the vector U_N provide the approximations to the exact solution of (28) at the collocation points, whereas the elements $(U_N)_{2j}$ approximate $\dot{x}(t_j)$ (see Fig. 4).

We observe that initially the errors achieved by M4 and M6 are similar to those committed by M2. This feature can be explained by the fact that the initial function does not satisfy the differential equation. After several subintervals, however, the accuracy actually improves and remains so for the integration interval considered.

As a final test, we illustrate how our numerical algorithm can also be used to determine with high accuracy the stability of a system modeled by Eq. (28), and in particular the stability boundaries in the parameter space, such as are presented in the stability chart of [2, Fig. 2.10]. To this end we fix $\delta = 2$ and $\varepsilon = 1$. Then it can be shown that there exists a value of $b \approx 0.71$ for which the dominant multiplier is $\mu = 1$. Specifically, the spectral collocation method of [1] with $N = 20$ provides $b = 0.706833720464083$. That this is not the correct value (up to machine accuracy) can be seen either by increasing N with the same algorithm or by applying the technique of [31], resulting instead in $b = 0.7068337166604264$. For this value of b, the algorithm proposed here with $N = 20$ and the 6th-order Magnus integrator with $M = 40$ provides the characteristic multiplier with an error $\approx 5.34 \cdot 10^{-12}$, in contrast with an error $\approx 5.38 \cdot 10^{-9}$ for the procedure of [1] also with the same number of collocation points $N = 20$.

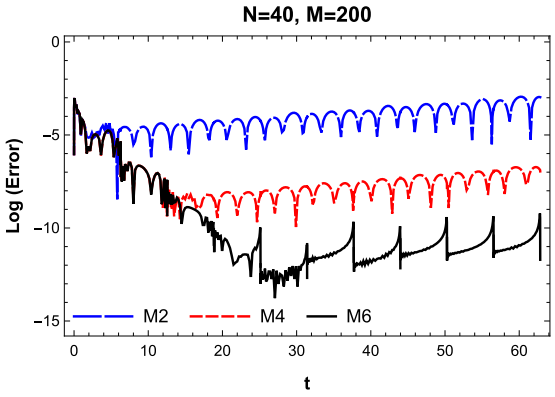

Fig. 4. Mean error in the solution of the delayed Mathieu equation (28) with $\delta = 1.5$, $\varepsilon = 0.5$, $b = -0.2$ and initial function $\phi(t) = t$ obtained by M2, M4 and M6 in the interval $[0, 20\pi]$ with $N = 40$, $M = 200$.

5. Extension to quasilinear problems

The algorithm we have presented in the previous section is mainly addressed to linear DDEs, both autonomous and explicitly time-dependent. It turns out, however, that the same procedure can also be adapted to the quasilinear delay Eq. (3), which we write again here for convenience:

$$\begin{aligned} &\frac{dx}{dt} = A\big(x(t-\tau)\big)\, x(t), \quad t \geq 0 \\ &x(t) = \phi(t), \qquad -\tau \leq t \leq 0. \end{aligned} \tag{30}$$

This problem can be formally stated as

$$\begin{aligned} &\frac{d}{dt}\tilde{u}(t) = Q(t)\tilde{u}(t), \qquad t \geq 0 \\ &\tilde{u}(0) = \phi(0) \end{aligned}$$

in terms of the function $\tilde{u} : [-\tau, \infty) \longrightarrow X$

$$\tilde{u}(t) \equiv \begin{cases} \phi(t), & t \in [-\tau, 0] \\ x(t), & t \in [0, \infty) \end{cases}$$

and the operator $Q(t) \equiv A(x(t-\tau))$ for $t \geq 0$ [20]. By judiciously approximating Q and the integrals involved in the Magnus expansion, it is possible to devise a 2nd-order integrator with good preservation properties [3]. The analysis has been generalized in [20] to more general classes of problems where A depends in a more involved way of the τ-history $x_t(\theta) = x(t+\theta)$. Achieving higher orders of convergence with this procedure, however, is more difficult and in fact it is left as an open problem in [20].

In the following, we show how the same procedure we have applied in the linear case can be generalized also in this setting, leading to very accurate numerical integrators. As before, we discretize the initial function $\phi(t)$ with Chebyshev collocation points in the interval $[-\tau, 0]$ and replace the abstract Cauchy problem with the $d(N+1)$-dimensional autonomous system

$$\begin{aligned} &\dot{U}_N(t) = \mathcal{A}_N(U_N)\, U_N(t), \quad t \geq 0 \\ &U_N(0) = \phi_N \end{aligned} \tag{31}$$

where

$$\mathcal{A}_N(U_N) = \begin{pmatrix} A((U_N)_{N+1}) & 0_d & \cdots & 0_d & 0 \\ & & \frac{2}{\tau}[\mathbb{D}^{(d+1,d(N+1))}] & & \end{pmatrix}. \tag{32}$$

In other words, we replace in (15) $A(t)$ by the new A, and B by the zero matrix. Observe that, since the matrix A in Eq. (30) only depends on $x(t-\tau)$, then the dependence of the matrix $\mathcal{A}_N$ in the discretized system (31) comes only through the last d components of the vector U_N, corresponding to the $(N+1)$-th collocation point. This is the meaning of the notation $A((U_N)_{N+1})$ in (32).

Next, the nonlinear initial value problem (32) is solved with exponential integrators based on a generalized Magnus expansion. In fact, it is shown in [32] how methods up to order four in this class can be obtained for nonlinear equations of the form

$$\dot{y} = \hat{A}(t, y)\, y, \qquad y(0) = y_0. \tag{33}$$

As in the linear case, the starting point is to represent the solution in the form $y(t) = \exp(\Omega(t))y_0$. Then, $\Omega(t)$ can be obtained by Picard's iteration as

$$\begin{aligned} &\Omega^{[0]}(t) \equiv 0 \\ &\Omega^{[m+1]}(t) = \int_0^t \sum_{k=0}^{\infty} \frac{B_k}{k!} \mathrm{ad}^k_{\Omega^{[m]}(s)} \hat{A}\big(s, \mathrm{e}^{\Omega^{[m]}(s)} y_0\big) ds, \qquad m \geq 0 \end{aligned} \tag{34}$$

so that $\lim_{m\to\infty} \Omega^{[m]}(t) = \Omega(t)$ for sufficiently small values of t. If terms up to $k = m-2$ are kept in (34), then

$$\Omega^{[m]}(t) = \Omega(t) + \mathcal{O}(t^{m+1}),$$

so that by appropriate quadratures, it is then possible to get consistent approximations for the first values of m. In particular, one can construct the following schemes of order 2 and 3, whereas the explicit algorithm for the method of order 4 can be found in [32,33]. For simplicity, we only consider the autonomous case in (33).

Order 2. Applying the trapezoidal rule to $\Omega^{[2]}$, one gets

$$\begin{aligned} u &= h\hat{A}(y_k) \\ v &= \frac{1}{2}\left(u + h\hat{A}(\mathrm{e}^u y_k)\right) \\ y_{k+1} &= \mathrm{e}^v y_k \end{aligned} \tag{35}$$

Order 3. Now one has to approximate the integrals appearing in $\Omega^{[1]}$, $\Omega^{[2]}$, and $\Omega^{[3]}$. The minimum number of evaluations of $\hat{A}$ and commutators is achieved by the following sequence:

$$\begin{aligned} Q_1 &= h\hat{A}(y_k) \\ Q_2 &= h\hat{A}(\mathrm{e}^{\frac{1}{2}Q_1} y_k) - Q_1 \\ u_1 &= \frac{1}{2}Q_1 + \frac{1}{4}Q_2 \\ u_2 &= Q_1 + Q_2 \\ Q_3 &= -u_2 + h\hat{A}(\mathrm{e}^{u_1} y_k) \\ Q_4 &= -u_2 - Q_2 + h\hat{A}(\mathrm{e}^{u_2} y_k) \\ u_3 &= u_2 + \frac{2}{3}Q_3 + \frac{1}{6}Q_4 - \frac{1}{6}[Q_1, Q_2] \\ y_{k+1} &= \mathrm{e}^{u_3} u_k \end{aligned} \tag{36}$$

Notice that these Magnus integrators require more computational effort than the corresponding schemes for the linear case.

In the following we check the whole procedure on two additional numerical examples. As before, the different integrators are denoted by M2, M3 and M4, respectively.

Example 3: a scalar nonlinear equation. The scalar equation (26) constitutes a particularly simple example of a quasilinear DDE of type (3) where the previous algorithm can be checked, since the exact solution is known explicitly, namely $z(t) = \mathrm{e}^{\sin t}$. To do that, we integrate the resulting N-dimensional system (31)–(32) from a discretization based on N Chebyshev collocation points (since $d = 1$ here) until the final time $t_f = \tau = \frac{\pi}{2}$. As in Example 1, we compute the mean error (29) in the interval as a function of M for $N = 10, 20, 30$ to check that the Magnus integrators provide indeed the prescribed order. In this way we get Fig. 5. Notice that, whereas the order of M2 is clearly visible even for large time steps, the accuracy of M4 only manifests itself for a sufficiently large number of Chebyshev points and very small step sizes. Otherwise, the results given by M3 and M4 are quite similar.

Example 4: a SIR model with delay. In Ref. [3], a 2nd-order numerical integrator also based on the Magnus expansion is proposed an tested on a widely used delayed SIR model (see [3] and references therein), namely

$$\begin{aligned} \dot{S}(t) &= -\beta S(t) \frac{I(t-\tau)}{1+\alpha I(t-\tau)} \\ \dot{I}(t) &= \beta S(t) \frac{I(t-\tau)}{1+\alpha I(t-\tau)} - \gamma I(t) \\ \dot{R}(t) &= \gamma I(t). \end{aligned} \tag{37}$$

It describes an epidemic model where the variation in the number of susceptible, $S(t)$, and infected, $I(t)$, individuals depend not only on the actual values of $S(t)$ and $I(t)$ respectively, but also on how many infected individuals they interacted a latent period before, i.e., at $t-\tau$. Notice that this is not the case for $R(t)$, the number of recovered individuals.

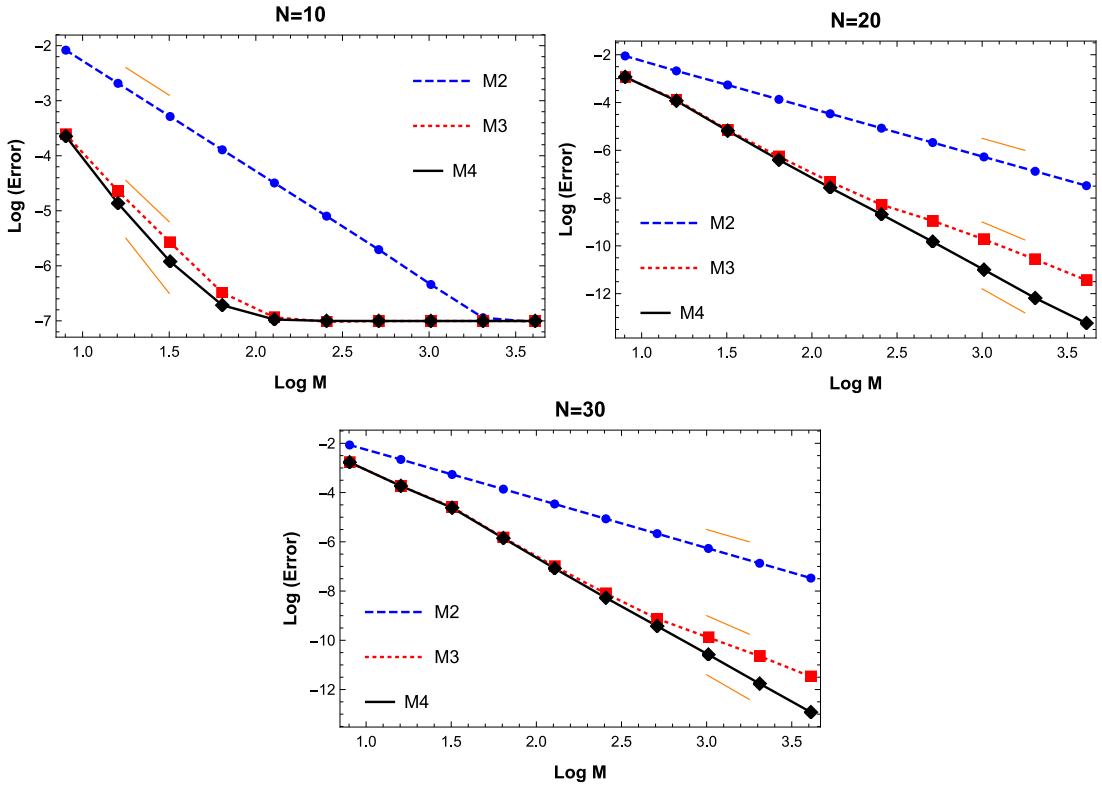

Fig. 5. Mean error in the solution obtained with Magnus integrators M2, M3 and M4 for the scalar nonlinear equation (26). Top left: $N = 10$. Top right: $N = 20$, Bottom: $N = 30$. The small segments correspond to orders 2, 3 and 4.

In (37), $\beta > 0$ and $\gamma > 0$ denote the infection and recovery rates, respectively, whereas $\alpha = 0$ if there is only a bilinear incidence rate, and $\alpha = 1$ if the model incorporates a saturated incidence rate [3].

System (37) can be expressed as Eq. (30) with $x = (S, I, R)^T$ and

$$A(x(t-\tau)) = \begin{pmatrix} -q(I(t-\tau)) & 0 & 0 \\ q(I(t-\tau)) & -\gamma & 0 \\ 0 & \gamma & 0 \end{pmatrix}, \tag{38}$$

where $q(I(t-\tau)) = \frac{I(t-\tau)}{1+\alpha I(t-\tau)}$. As in [3], we take $\alpha = 0$, $\beta = 1$, $\gamma = 1$, latent period $\tau = 1$, initial values $S_0 = 0.7$, $I_0 = 0.2$, $R_0 = 0.1$ and initial function

$$\phi(t) = I_0 - \frac{1}{2}t,$$

for which the effect of the latent period is most evident. Then we integrate numerically with our algorithm until the final time $t_f = 4\tau$ and compute the relative error

$$E_r = \frac{\|x(t_f) - x_n(t_f)\|}{\|x(t_f)\|},$$

where the reference solution $x(t_f)$ is obtained with the Matlab built-in function `dde23` with relative tolerance 10^{-12} and $x_n(t_f)$ refers to the numerical solution computed with Magnus integrators (as appropriately extracted from the whole vector $U_N(t_f)$). For this particular example M3 already provides order 4, as shown in Fig. 6, and so we do not include M4 in the graphs. The accuracy achieved by M3 is worth remarking: with $h = 0.01$ (corresponding to $M = 100$) the relative error is approximately 10^{-9}. Now we get errors smaller than 10^{-2} with the largest possible value of the time step size, namely $h = \tau$. Increasing the number N leads to a better accuracy, but the relative behavior is similar.

We have included in the last graph ($N = 60$), and for comparison, the results achieved with the code RETARD[1] in a Matlab implementation. It is a modification of the code DOPRI5 (Runge–Kutta method of Dormand & Prince of order 5(4) with dense output and variable step size), which is very efficient for delay differential equations [34]. The points forming

[1] https://www.unige.ch/~hairer/software.html

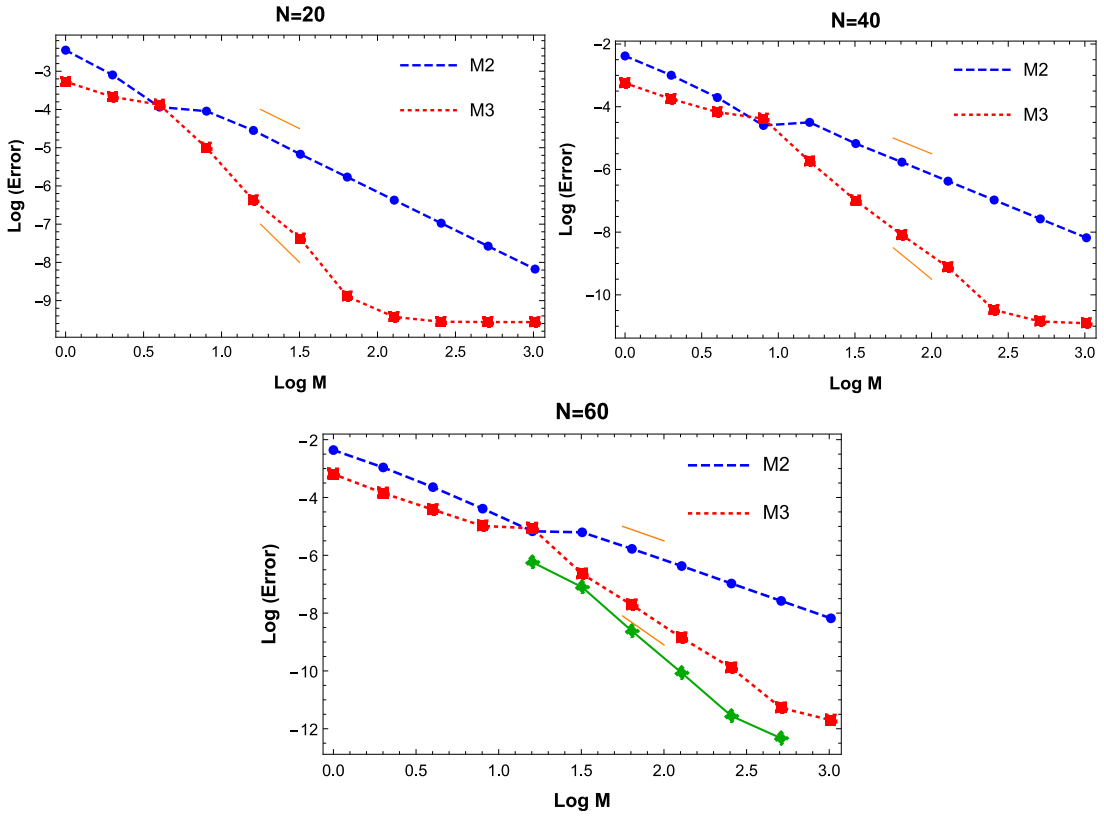

Fig. 6. Relative error in the solution obtained with M2 and M3 for the SIR model with delay (37). Top left: $N = 20$ top right: $N = 40$, bottom: $N = 60$. The small segments correspond to orders 2 and 4. In this case M3 already provides order 4. In the bottom graph we also include the result obtained by the code RETARD based on the Runge–Kutta Dormand & Prince method of order 5 with dense output and variable step size (green line with crosses).

the green line have been obtained by fixing a maximal step size $h_{\max}$ so that when selecting h along the integration one always has $h \leq h_{\max}$. Specifically, $h_{\max} = 5 \cdot 2^{-n}$, $n = 3, \ldots, 8$. We see that the result furnished by M3 (of nominal order 3) is comparable with RETARD (order 5) with this restriction on the maximal step size.

Finally, in Fig. 7 we show the relative error as a function of time when the integration is carried out in the interval $[0, 10\tau]$ with the same values for the parameters, initial function

$$\phi(t) = I_0 + \frac{1}{2}t, \tag{39}$$

$N = 20$ collocation points and $M = h^{-1} = 20$. In this case, no secular growth in the error is observed, with M3 providing more accurate results.

Preservation of properties. Since model (37) deals with a population, it is clear that $S(t)$, $I(t)$ and $R(t)$ are non-negative for all $t \geq 0$, and moreover $S(t)+I(t)+R(t)$ is constant. This feature is connected with the special structure the corresponding matrix $A(x(t-\tau))$ possesses in this case: in fact, A is a graph Laplacian, characterized by the following properties [35]:

- its elements $A_{k,l}$ verify that $A_{k,l} \geq 0$ for $k, l = 1, \ldots, d$, $k \neq l$, $A_{k,k} \leq 0$ for $k = 1, \ldots, d$;
- $\sum_{k=1}^{d} A_{k,l} = 0$ for $l = 1, \ldots, d$.

It is then natural to analyze whether the corresponding approximations obtained by our numerical algorithm also verify these properties.

One can hardly expect that the matrix $\mathcal{A}_N(U_N)$ in (31) inherits the special structure A may have in general, due to the presence of the differentiation matrix $\mathbb{D}^{(d+1,d(N+1))}$. One should take into consideration, however, the following key observations:

- the first d rows of $\mathcal{A}_N(U_N)$ are zero, except for the first d columns, where A is placed; in other words, the first $d \times d$ block of $\mathcal{A}_N(U_N)$ is precisely A;
- the exponential matrix $e^{\mathcal{A}_N}$ has the same structure as $\mathcal{A}_N$, and the first $d \times d$ block corresponds to e^A;

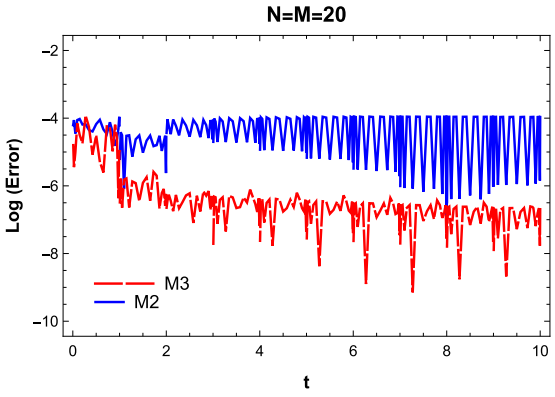

Fig. 7. Relative error as a function of time for the SIR model with delay (37) and $N = M = 20$. Parameters $\alpha = 0$, $\beta = 1$, $\gamma = 1$ and initial function (39). Final time: $t_f = 10\tau$.

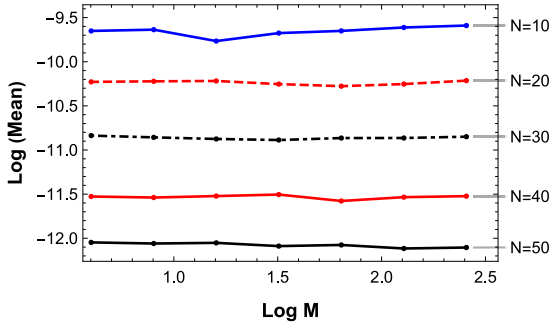

Fig. 8. Average value of the error in the total population (40) obtained with M3 for different values of N and M for the epidemic model (37). The parameters and initial condition are the same as in Fig. 6.

- the computations involved in the Magnus integrators (35) and (36) do not alter this structure of the matrices; in other words, the matrices obtained at the intermediate stages M2 and M3 ($u, v, Q_1, Q_2, \ldots, u_3$) have the same basic structure as $\mathcal{A}_N$;
- if all the elements of $w \in \mathbb{R}^d$ are non-negative, then all elements of $\mathrm{e}^u w$ are non-negative if u is graph Laplacian [3,35].

In consequence, by construction, the previous Magnus integrators preserve the total population and positivity unconditionally at times $t = n\tau, n = 1, 2, \ldots$ [35], whereas at intermediate times the error is dictated by the number of Chebyshev nodes used in the spectral discretization. This feature is clearly illustrated in Fig. 8, where we show the average value of

$$|S(\tau + \theta_j) + I(\tau + \theta_j) + R(\tau + \theta_j) - 1| \tag{40}$$

over the interval $[3\tau, 4\tau]$ obtained with the 3th-order Magnus integrator M3 with different Chebyshev points and increasingly large numbers of subdivisions M. Whereas at $t = \tau$, this difference is of the order of round-off, at intermediate steps it can be reduced significantly by increasing the number N of nodes. In all cases, the error does not grow with time.

6. Concluding remarks

We have presented a numerical procedure to integrate non-autonomous linear delay differential equations consisting of two main components. First, the use of a spectral discretization of the delayed part to transform the original problem into a linear ordinary differential equation (ODE) whose dimension depends on the number N of collocation points: thus, if the original matrix system has dimension d, then the transformed ODE has dimension $d(N + 1)$. Second, this system is then solved by applying numerical integrators based on the Magnus expansion. Thus, for sufficiently large values of N, approximate solutions up to order 6 have been obtained for linear systems. In fact, if the step size is small enough, then the final accuracy is dictated by N for schemes of order greater than two. The idea of formulating the original DDE as an abstract Cauchy problem in terms of an operator $\mathcal{A}$ which is then discretized by pseudo-spectral collocation techniques is certainly not new. In fact it has been successfully applied not only in the context of delay differential equations, but also for other classes of nonlinear delay problems, to analyze the stability of the original problem, compute periodic solutions and obtain bifurcation diagrams. Here, by contrast, we propose to integrate numerically in time the resulting ODE system

by methods based on the classical Magnus expansion. These have proved to be a successful alternative to other standard procedures for non-autonomous linear differential equations, especially when they possess qualitative properties which should be preserved by the numerical approximation.

The technique is thus different from the standard approach based on the use of a discrete method for ODEs (e.g., a Runge–Kutta scheme) endowed with some interpolant, and it is particularly flexible for this type of equations. In particular, it allows one to adjust the step size and even the order of the Magnus method along the integration, according with a specified tolerance, as shown in [24,32,33].

The collected examples (and others not included here) show that the combination of Magnus integrators with the standard approach of discretizing the associated abstract Cauchy problem with pseudo-spectral collocation leads indeed to very accurate results when the number of points for spectral discretization is sufficiently large.

This work may be considered as a first stage in a more comprehensive treatment, since there are several aspects of the procedure that need to be further clarified. We can mention, in particular, the smoothness of the solution of the reduced ODE or whether the initial function belongs to the domain of the operator $\mathcal{A}$ in the abstract Cauchy problem. Here our starting hypothesis is that the abstract Cauchy problem can be discretized by pseudo-spectral techniques to get a system of ODEs. This system is subsequently solved numerically by applying integrators based on the classical Magnus expansion. In a sense, Magnus expansion constitutes the natural generalization of the exact (formal) solution of the autonomous system (9). On the other hand, one should notice that it involves (iterated) integrals in its formulation, and so the requirements of smoothness can be relaxed with respect, e.g., to Runge–Kutta methods. This has been illustrated in several standard references on the Magnus expansion and Magnus integrators [21,22].

Whereas a rigorous error analysis along the line of e.g. [1] is still lacking (and might be difficult to carry out, as the treatment done in [20] for a second order integrator clearly shows), we believe the results collected here provide a sufficiently convincing evidence of the capabilities that Magnus integrators possess in combination with the abstract Cauchy problem formulation.

Although only one delay has been considered here, the generalization to k distinct delays is straightforward. We have also extended the treatment to quasilinear delay equations of the form (3), this time in combination with integrators based on the Magnus expansion for nonlinear equations. The treatment of the epidemic model with delay (37) shows that the algorithm preserves unconditionally important features of the system, such as the total population and the positivity of the variables at times $t = n\tau$, whereas error at intermediate times is governed by the number of nodes N, which in any case remains constant.

The use of integrators based on the Magnus expansion involves the computation of the exponential of matrices of dimension $d(N+1) \times d(N+1)$, and this is very often the most expensive part of the algorithm. In this respect, it is worth remarking that the number N of collocation points is not very large (in our examples we get excellent results already with $N = 20$ or $N = 30$), and that we use the technique presented in [25] to approximate the exponential by conveniently chosen Taylor polynomials. In this way the computational cost is reduced with respect to standard algorithms based on Padé approximants.

Data availability

No data was used for the research described in the article.

Acknowledgments

This work has been supported by Ministerio de Ciencia e Innovación (Spain) through projects PID2019-104927GB-C21, and PID2021-124577NB-100, MCIN/AEI/10.13039/501100011033, ERDF (“A way of making Europe”). Additional support has been received from Universitat Jaume I through project UJI-B2022-19. The authors wish also to thank the two referees for their suggestions, which have contributed to improve this work.

References

[1] D. Breda, S. Maset, R. Vermiglio, Stability of Linear Delay Differential Equations. A Numerical Approach with MATLAB, Springer, 2015.
[2] T. Insperger, G. Stépán, Semi-Discretization for Time-Delay Systems, Springer, 2011.
[3] P. Csomós, Magnus-type integrator for semilinear delay equations with an application to epidemic models, J. Comput. Appl. Math. 363 (2020) 92–105.
[4] G.E. Hutchinson, Circular causal systems in ecology, Ann. New York Acad. Sci. 50 (1948) 221–246.
[5] A. Bellen, M. Zennaro, Numerical Methods for Delay Differential Equations, Oxford University Press, 2003.
[6] A. Bellen, S. Maset, Numerical solution of constant coefficient linear delay differential equations as abstract Cauchy problems, Numer. Math. 84 (2000) 351–374.
[7] S. Maset, Asymptotic stability in the numerical solution of linear pure delay differential equations as abstract Cauchy problems, J. Comput. Appl. Math. 111 (1999) 163–172.
[8] E. Butcher, O. Bobrenkov, On the Chebyshev spectral continuous time approximation for constant and periodic delay differential equations, Commun. Nonlinear Sci. Numer. Simul. 16 (2011) 1541–1554.
[9] J.-Q. Sun, A method of continuous time approximation of delayed dynamical systems, Commun. Nonlinear Sci. Numer. Simul. 14 (2009) 998–1007.

[10] D. Breda, O. Diekmann, M. Gyllenberg, F. Scarabel, R. Vermiglio, Pseudospectral discretization of nonlinear delay equations: new prospects for numerical bifurcation analysis, SIAM J. Appl. Dyn. Syst. 15 (2016) 1–23.
[11] D. Breda, S. Maset, R. Vermiglio, Approximation of eigenvalues of evolution operators for linear retarded functional differential equations, SIAM J. Numer. Anal. 50 (2012) 1456–1483.
[12] F. Borgioli, D. Hajdu, T. Insperger, G. Stepan, W. Michiels, Pseudospectral method for assessing stability robustness for linear time-periodic delayed dynamical systems, Internat. J. Numer. Methods Engrg. 121 (2020) 3505–3528.
[13] D. Breda, D. Liessi, R. Vermiglio, Piecewise discretization of monodromy operators of delay equations on adapted meshes, J. Comput. Dyn. 9 (2022) 103–121.
[14] K. Engelborghs, T. Luzyanina, K.I.T. Hout, D. Roose, Collocation methods for the computation of periodic solutions of delay differential equations, SIAM J. Sci. Comput. 22 (2000) 1593–1609.
[15] J. Hale, S.V. Lunel, Introduction To Functional Differential Equations, Springer, 1993.
[16] K.-J. Engel, R. Nagel, One-Parameter Semigroups for Linear Evolution Equations, Springer, 2000.
[17] L. Trefethen, Spectral Methods in MATLAB, SIAM, 2000.
[18] C. Chicone, Y. Latushkin, Evolution Semigroups in Dynamical Systems and Differential Equations, American Mathematical Society, 1999.
[19] G. Nickel, Evolution semigroups for nonautonomous cauchy problems, Abstr. Appl. Anal. 2 (1997) 73–95.
[20] P. Csomós, D. Kunszenti-Kovács, A second-order Magnus-type integrator for evolution equations with delay, IMA J. Numer. Anal. (2022) http://dx.doi.org/10.1093/imanum/drac060.
[21] A. Iserles, H. Munthe-Kaas, S. Nørsett, A. Zanna, Lie-group methods, Acta Numer. 9 (2000) 215–365.
[22] S. Blanes, F. Casas, J. Oteo, J. Ros, The Magnus expansion and some of its applications, Phys. Rep. 470 (2009) 151–238.
[23] A. Arnal, F. Casas, C. Chiralt, A general formula for the magnus expansion in terms of iterated integrals of right-nested commutators, J. Phys. Commun. 2 (2018) 035024.
[24] S. Blanes, F. Casas, J. Ros, Improved high order integrators based on the Magnus expansion, BIT 40 (2000) 434–450.
[25] P. Bader, S. Blanes, F. Casas, Computing the matrix exponential with an optimized Taylor polynomial approximation, Mathematics 7 (2019) 1174.
[26] P. Bader, S. Blanes, F. Casas, M. Seydaoğlu, An efficient algorithm to compute the exponential of skew-Hermitian matrices for the time integration of the Schrödinger equation, Math. Com. Simul. 194 (2022) 383–400.
[27] C. González, A. Ostermann, M. Thalhammer, A second-order magnus-type integrator for nonautonomous parabolic problems, J. Comput. Appl. Math. 189 (2006) 142–156.
[28] M. Hochbruck, C. Lubich, On magnus integrators for time-dependent Schrödinger equations, SIAM J. Numer. Anal. 41 (2004) 945–963.
[29] S. Blanes, F. Casas, J. Ros, High order optimized geometric integrators for linear differential equations, BIT 42 (2002) 262–284.
[30] S. Yanchuk, S. Ruschel, J. Sieber, M. Wolfrum, Temporal dissipative solitons in time-delay feedback systems, Phys. Rev. Lett. 123 (2019) 053901.
[31] T. Insperger, G. Stépán, Stability chart for the delayed Mathieu equation, Proc. R. Soc. Lond. Ser. A Math. Phys. Eng. Sci. 458 (2002) 1989–1998.
[32] F. Casas, A. Iserles, Explicit magnus expansions for nonlinear equations, J. Phys. A: Math. Gen. 39 (2006) 5445–5461.
[33] M. Hajiketabi, F. Casas, Numerical integrators based on the Magnus expansion for nonlinear dynamical systems, Appl. Math. Comput. 369 (2020) 124844.
[34] E. Hairer, S. Nørsett, G. Wanner, Solving Ordinary Differential Equations I. Nonstiff Problems, second ed., Springer, 1993.
[35] S. Blanes, A. Iserles, S. Macnamara, Positivity-preserving methods for ordinary differential equations, ESAIM Math. Model. Numer. Anal. 56 (6) (2022) 1843–1870.